

## INTERACTION OF GOLD NANOPARTICLES WITH RAT BRAIN SYNAPTOSOMAL PLASMA MEMBRANE $\text{Na}^+/\text{K}^+$ -ATPase AND $\text{Mg}^{2+}$ -ATPase

VOIN PETROVIĆ, VESNA VODNIK, IVANA STANOJEVIĆ,  
ZLATKO RAKOČEVIĆ, VESNA VASIĆ\*

*Vinča Institute of Nuclear Sciences, University of Belgrade, PO Box 522,  
Belgrade, Serbia*

The aim of the work was to investigate the interaction between borate capped gold nanoparticles (NPs) and the rat brain synaptosomal plasma membranes (SPM), as well as the effects of these NPs on SPM  $\text{Na}^+/\text{K}^+$ -ATPase and  $\text{Mg}^{2+}$ -ATPase activity. The changes in the UV-vis spectra of NPs and SPM assembly suggested the agglomeration and precipitation of NPs. FTIR measurements indicated that both protein  $-\text{SH}$  and  $-\text{NH}_2$  groups and positively charged membrane fragments were implicated in the adhesion of SPM to the surface of NPs. AFM showed an increase in the particularization of the SPM material after mixing with gold NPs. Influence of gold NPs on  $\text{Na}^+/\text{K}^+$ -ATPase and  $\text{Mg}^{2+}$ -ATPase activity was investigated as the function of NPs and protein concentration, preincubation time and also in the presence of various concentrations of ouabain, the specific enzyme inhibitor. NPs induced the stimulation of  $\text{Na}^+/\text{K}^+$ -ATPase activity for more than 100%, since  $\text{Mg}^{2+}$ -ATPase activity remained unaffected. We propose that this stimulation of enzyme activity was a consequence of an increase of the active surface of membranes.

(Received February 24, 2012; Accepted March 20, 2012)

*Keywords:* Gold nanoparticles,  $\text{Na}^+/\text{K}^+$ -ATPase,  $\text{Mg}^{2+}$ -ATPase, synaptosomal plasma membranes, biofunctionalization.

### 1. Introduction

Gold nanoparticles (Au NPs) are a very attractive tool in biomedical research, because they have repeatedly shown great potential as substance carriers, active surfaces and even biologically active agents [1]. Since they can be readily taken up by cells [2], they are proposed in the medical sector as new tools in diagnostics [3] and drug delivery systems [4]. Although GNPs are considered being inert in biomedical applications [5], the size dependent cytotoxicity towards different cell types, with smaller particles being more toxic has been reported [6, 7].

The particles themselves are easily modified due to the gold's ability to bond with biologically important molecular groups such as amines, thiols, and carboxyl groups from amino acids and proteins [8, 9]. They have also been used as immobilization matrices for enzymes, where the immobilized enzyme was found to be more stable compared to free enzyme [10, 11]. Of all available molecular targets in living tissue, proteins have shown the greatest affinity towards GNPs. The conjugation of proteins with GNPs stabilized the system and also introduced biocompatible functionalities into the nanoparticles for further biological application. [12-14] The binding of the proteins to nanoparticles might occur by electrostatic forces between the surface-terminated negatively charged groups capping the nanoparticle and the positively charged functional groups of the protein (e.g. aminoacids residues) [9, 15, 16].

---

\*Corresponding author: evasic@vinca.rs

$\text{Na}^+/\text{K}^+$ -ATPase and  $\text{Mg}^{2+}$ -ATPase (ecto-ATPase) are membrane enzymes ubiquitous in animal cells that involve 5'-adenosine triphosphate (ATP) as a substrate for their functioning.  $\text{Na}^+/\text{K}^+$ -ATPase plays a key role in the active transport of monovalent cations ( $\text{Na}^+$  and  $\text{K}^+$ ) across the membrane [17]. Beside its transporter function,  $\text{Na}^+/\text{K}^+$ -ATPase acts as the receptor for cardiac glycosides such as ouabain like compounds [18], which are the specific inhibitors of the enzyme. The enzyme is composed of  $\alpha$ -subunit, which contains the adenosinetriphosphate (ATP),  $\text{Na}^+$ ,  $\text{K}^+$  and ouabain binding sites, as well as the site for phosphorylation and  $\beta$ -subunit, which stabilizes the  $\text{K}^+$  binding cage. The ouabain insensitive ecto-adenosine triphosphatase ( $\text{Mg}^{2+}$ -ATPase) represents an integral membrane protein that, in the presence of divalent cations ( $\text{Ca}^{2+}$  or  $\text{Mg}^{2+}$ ), hydrolyses extracellular nucleotides because of the outward orientation of its active site [19]. It is much less well characterized than sodium pump, but apparently consists of at least two forms with different molecular weights and sensitivity to metal ions. There is a great number of organic molecules and metallic ions that can modulate the activity of these enzymes [20, 21]. Literature surveys suggest that some NPs (Cu,  $\text{TiO}_2$ ) inhibit  $\text{Na}^+/\text{K}^+$  ATPase activity and induce oxidative stress [22, 23]. Also, it was shown that some of the gold compounds have an inhibitory effect upon enzyme [24]. On the contrary, the literature data indicate that gold and silver nanoparticles stimulated ATPases activity of native and rehydrated cells of *Escherichia coli* [25]. In general, there are some fundamental differences between the physiological effects of metal ions and NPs. The chemistry and behavior of metal nanoparticles involve dynamic aspects of aggregation theory, rather than equilibrium models traditionally used for free metal ions.

One of the available model systems for the study of  $\text{Na}^+/\text{K}^+$ -ATPase and  $\text{Mg}^{2+}$ -ATPase are the rat brain synaptosomal plasma membrane fragments (SPM) [26]. In this paper we describe the influence of borate capped Au NPs of various sizes on SPM  $\text{Na}^+/\text{K}^+$ -ATPase and  $\text{Mg}^{2+}$ -ATPase activity in this model system. In addition, the interaction of SPM with Au NPs was characterized by application of various techniques, such as UV-Vis spectrophotometry, Fourier transformation infrared spectroscopy (FTIR) and atomic force microscopy (AFM).

## 2. Experimental

### 2.1 Materials

Gold (III) chloride trihydrate ( $\text{HAuCl}_4 \times 3\text{H}_2\text{O}$ ), sodium borohydride ( $\text{NaBH}_4$ , 99%), perchloric acid ( $\text{HClO}_4$ ), ouabain, all from Aldrich, were used as received. Rat SPM were isolated according to a previously described method and stored at  $-80^\circ\text{C}$  until use [26]. Adenosinetriphosphate (ATP), sodium chloride ( $\text{NaCl}$ ), potassium chloride ( $\text{KCl}$ ), magnesium chloride ( $\text{MgCl}_2$ ), tris(hydroxymethyl) aminomethane ( $\text{TrisHCl}$ ), were purchased from Sigma Aldrich (Germany). Stannous chloride ( $\text{SnCl}_2$ ) and ammonium heptamolybdate ( $(\text{NH}_4)_6\text{Mo}_7\text{O}_{24}$ ) were from Merck (Darmstadt, Germany). Water purified with a Millipore Milli-Q water system was used for preparing all solutions.

### 2.2 Preparation of gold nanoparticles

Au NPs were obtained by the reduction of  $\text{HAuCl}_4$  with  $\text{NaBH}_4$ . Precisely, 100 mL of 0.2 mM  $\text{HAuCl}_4$  was reduced by 5.3 mM of  $\text{NaBH}_4$  at room temperature, to yield a ruby-red solution. The calculated value of NPs concentration was  $2.8 \times 10^{-9}$  M, assuming that the reduction from gold(III) to gold atoms was 100% complete.

### 2.3 ATPase activity measurements

The incubation mixture contained 400 mM  $\text{NaCl}$ ; 80 mM  $\text{KCl}$ ; 20 mM  $\text{MgCl}_2$ , 200 mM  $\text{Tris HCl}$ ,  $\text{pH}=7.4$  and  $25\mu\text{L}$  of SPM containing 1 mg/mL protein in total volume  $200\mu\text{L}$  at  $37^\circ\text{C}$ .  $20\mu\text{L}$  of 20 mM ATP was added to initiate the enzymatic reaction which was allowed to proceed for 15 min. Reaction was stopped by an addition of  $22\mu\text{L}$  of 3 M  $\text{HClO}_4$  and by cooling of samples on ice. The concentration of liberated inorganic orthophosphate was determined

spectrophotometrically [26]. The activity obtained without NaCl and KCl in the medium assay was attributed to  $Mg^{2+}$ -ATPase.  $Na^+/K^+$ -ATPase activity was calculated as a difference between the total ATPase and  $Mg^{2+}$ -ATPase activity. The results represent the mean values of at least two experiments done in duplicate.

#### 2.4 Apparatus

Transmission electron microscope (TEM, JOEL 100CX) was used to observe the morphology and average size of Au nanoparticles.

All spectrophotometric measurements were performed on a Perkin Elmer Lambda 35 UV-vis spectrophotometer with 1 cm path length quartz cuvette.

FTIR spectra were recorded on Thermo Electron Corporation Nicolet 380 FTIR Spectrophotometer with ATR (Attenuated Total Reflection) accessory, equipped with a diamond tip, in the region between 4000 and 500  $cm^{-1}$ .

AFM measurements were carried out using commercial AFM VECCO Quadrex Multi Mmode IIIE equipment operating in tapping mode (TMAFM) on highly oriented pyrolytic graphite (HOPG). Surface topography and phase images were simultaneously acquired using a commercial NanoScience-Team Nanotec GmbH SCN (Solid Nitride Cone) AFM probe, with tip radius lower than 10 nm. AFM observations were repeated on different areas from  $2 \times 2 \mu m^2$  to  $250 \times 250 nm^2$  on the same substrate at ambient laboratory conditions (about 20°C)

Droplet-evaporation method was used for preparing AFM samples for analysis. A droplet of  $2 \times 10^{-9}$  M Au colloid or SPM containing 1 mg/mL of protein was deposited on freshly cleaned HOPG 1x1 cm. The droplet was then carefully washed after allowing the sample to sit about 15 minutes. For gold nanoparticles functionalized with protein, 100  $\mu L$  of Au colloid was mixed with 25  $\mu L$  of SPM. 15 min after mixing the sample was put on HOPG as described above.

### 3. Results

#### 3.1 Spectrophotometric characterization of Au NPs interaction with SPM

The Au colloidal dispersion was used to investigate the interaction with SPM. According to TEM measurements (data not shown), the nanoparticles were spherical in shape with the average particle diameter  $9.5 \pm 0.8$  nm.

UV-vis spectroscopy was initially used to monitor spectral changes in colloidal solutions upon addition of SPM. The spectra were recorded before and after the mixing of 100  $\mu l$  of SPM and 25  $\mu l$  of colloid solution containing  $2 \times 10^{-9}$  M NPs, under stirring at room temperature. This was then diluted with water to 1.5 mL and measured. The gold NPs show an intense surface plasmon resonance (SPR) band at 518 nm due to the collective excitation of conducting electrons in a metal (Fig. 1 curve 2).

Adding SPM into the gold colloidal solution, some spectral changes were observed. (Fig. 1 curves 3-5). The spectral changes of SPR band resulted from the replacement of borate ions on the NPs surface by the SPM molecules that caused a significant decrease in the stability ratio and aggregation of NPs. The agglomeration was extremely fast and fine precipitates were formed after 10 min of mixing with SPM. As a consequence of agglomeration, the corresponding SPR band was broadened and shifted to longer wavelengths due to dipole-dipole interactions of high induced dipole moment of NPs in aggregates. The SPR band completely disappeared after 20 min.

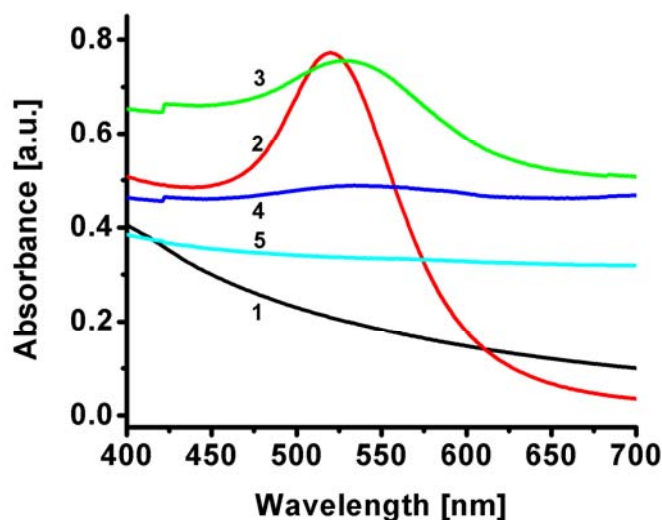


Fig. 1. UV-vis spectra of the solutions containing 66.6  $\mu\text{g/mL}$  SPM (1) and  $3.3 \times 10^{-11}$  M Au NPs (2) and 1 min (3), 10 min (4) and 20 min (5) after the mixing.

### 3.2 FTIR characterization of Au NPs with SPM

FTIR spectra were recorded in order to evaluate the possible types of interactions that exist between the Au NPs and SPM. A number of vibration bands can be seen in the two different regions of the spectra as shown in Fig. 2. The FTIR spectrum of the SPM in water solution exhibits small bands located at 2940-2820  $\text{cm}^{-1}$  related to the protein and lipid C-H asymmetric and symmetric stretching vibrations. The interaction Au NPs with SPM molecules leads to increase intensity and narrowing of the band at 2928  $\text{cm}^{-1}$  due to the asymmetric stretching mode of the methylene groups in lipid sequences. Also, the rigid chain conformation on the NPs surface restricts protein mobility, resulting in the narrowing of the stretching bands [27, 28].

The multiply bonded CO group provides the intense bands between 2100 and 1900  $\text{cm}^{-1}$ , clearly visible in the Fig.2. The new mode due to scissoring of a methylene group adjacent to the Au-S bond ( $\delta_s$ ) appears at 1430  $\text{cm}^{-1}$  together with the weak bands around 1320  $\text{cm}^{-1}$ . These bands are related to C-N, C-O vibrations of the protein backbone and amino acid residues and are shown in the spectrum. In addition, the weak band at 1050  $\text{cm}^{-1}$  can be attributed to vibrations involving interaction between C-O stretching and C-N stretching. This band is shifted to 1160  $\text{cm}^{-1}$ . Such effects are not surprising given the proximity of the gold surface to the bonds involved in these motions.

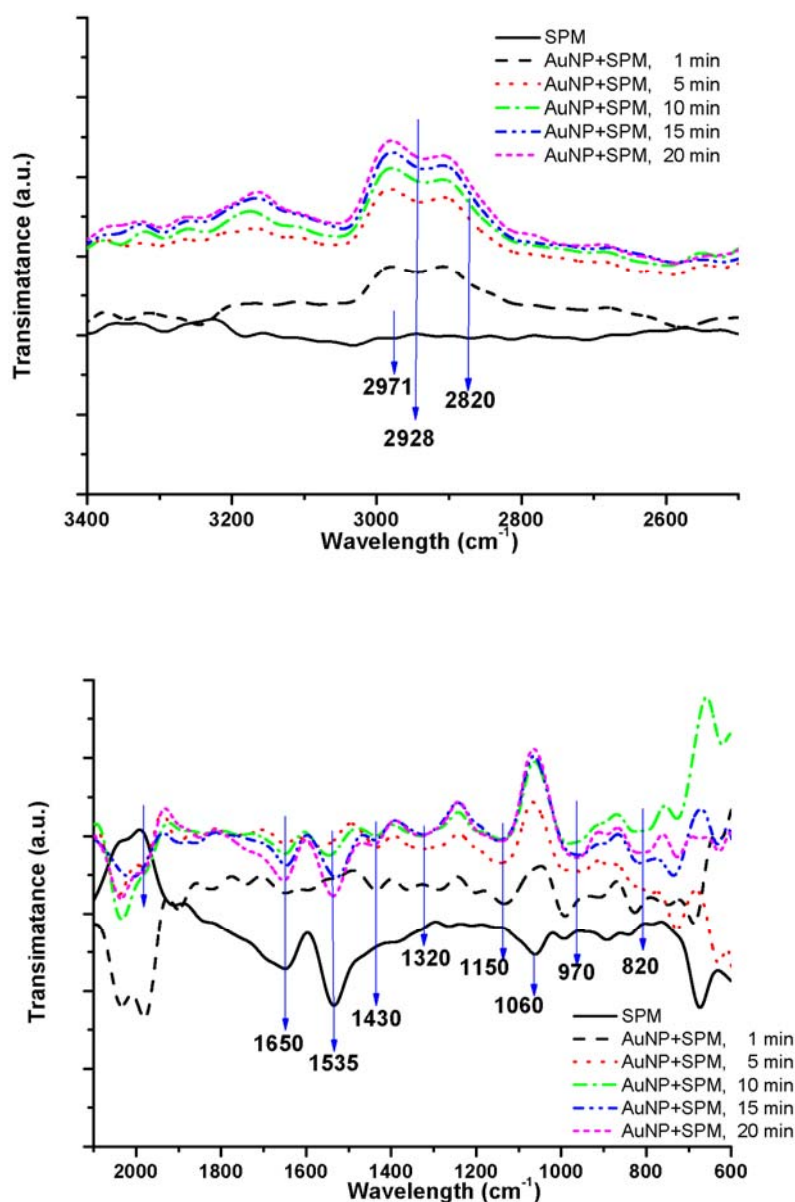


Fig. 2. FTIR spectra of SPM over time upon the addition of Au NPs

The specific region at  $600\text{--}700\text{ cm}^{-1}$  assigned to the  $\nu\text{S-C}$  symmetric stretching vibration shows significant changes together with the bands at  $970$  and  $820\text{ cm}^{-1}$  assigned to  $\nu\text{Au-S}$  symmetric stretching vibration, indicating that Au NPs and SPM interact via sulfur group [29]. The next characteristic vibration bands arise from the amide groups of proteins and provide information on its secondary structure, have been identified. Among them, amide I band ( $\text{C=O}$  stretching mode) appears at  $1650\text{ cm}^{-1}$  and the amide II band due to the coupling  $\text{C-N}$  stretch to  $\text{N-H}$  bending at  $1535\text{ cm}^{-1}$  [30]. The NPs interactions with SPM lead to increase intensity of these bands due to the interaction (via H-bonding) with protein  $\text{C=O}$  and  $\text{C-N}$  groups. Also, the slight displacement of the maximum amide I band from  $1650$  to  $1652\text{ cm}^{-1}$  and amide II band from  $1535$  to  $1537\text{ cm}^{-1}$  were observed upon addition of Au NPs.

### 3.3 AFM visualization of Au NPs interaction with SPM

The AFM measurements were performed with Au NPs in the absence and presence of SPM on HOPG. A representative AFM image of Au NPs in the absence of SPM is shown in Fig. 3. The section analysis of the image indicates the peaks, which correspond to the Au NPs anchored on the HOPG. The sizes of the particles were measured directly from AFM images. Single colloids display homogenous lateral and vertical dimensions. Height evolution was obtained by cross section profile in Fig. 3b. The size of nanoparticles (average diameter 9.4 nm) is in good agreement with the results obtained by TEM measurements.

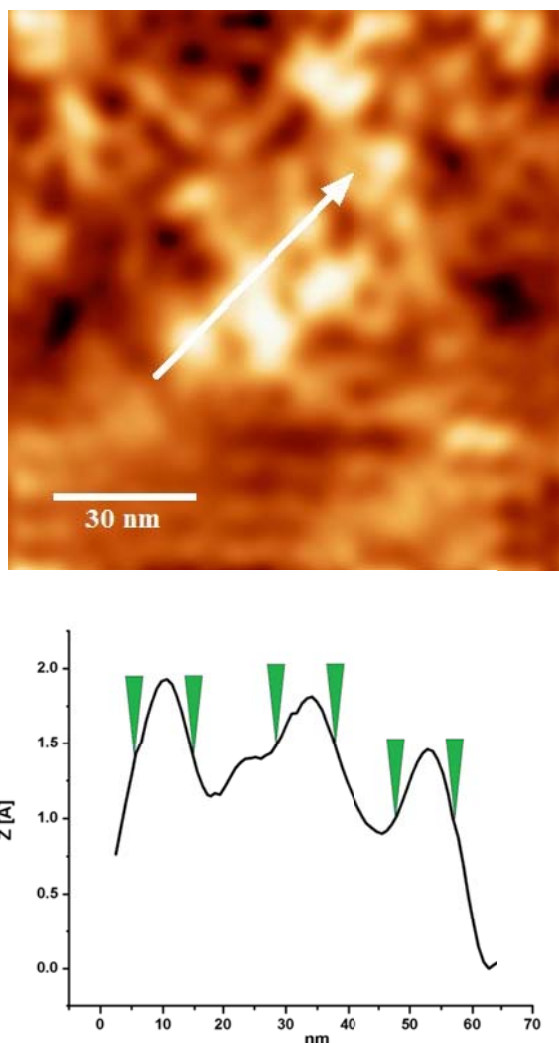


Fig. 3. AFM images of Au NPs deposited on HOPG after 15 min deposition time, scanned area  $250 \times 250 \text{ nm}^2$ ; a) 2D topography with cross section, b) cross section profile.

Fig. 4. shows the typical image of SPM membrane patches well distributed on the surface, in which the particles that are supposed to be membrane proteins are clearly observed. The stringy structure of SPM can be noticed.

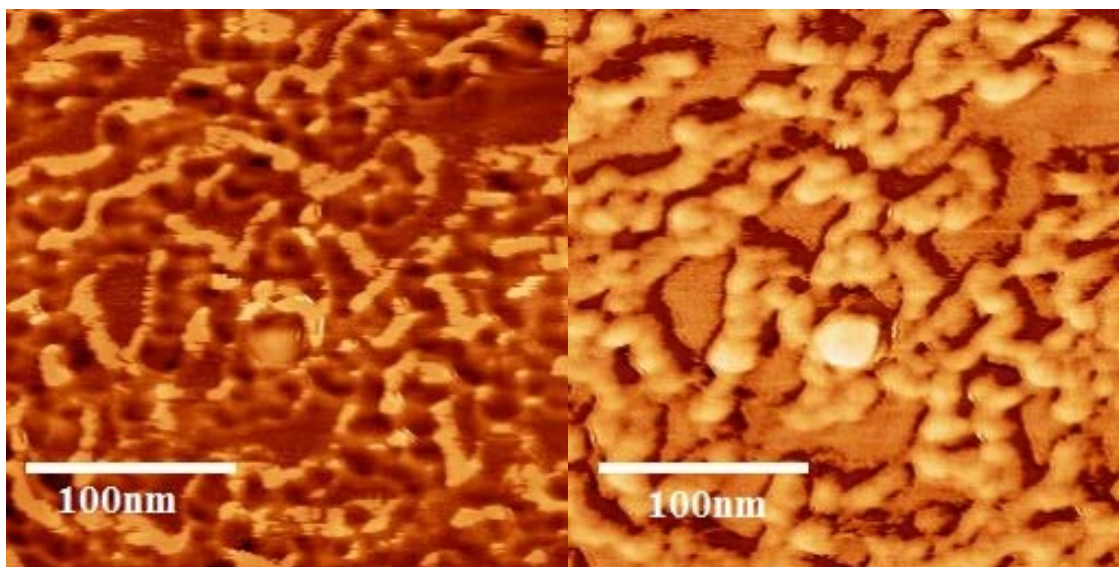


Fig. 4. AFM images of SPM deposited on HOPG after 15 min deposition time, scanned area  $250 \times 250 \text{ nm}^2$ ; a) - 2D topography, b) - 2D phase view.

Fig. 5. shows the mixture of SPM and Au NPs. It can be seen that there are no string-like structures and that most of the material is divided into smaller spherical aggregations. The results presented in Figs. 4 and 5 obtained from the AFM measurements indicated a change in the fine structure of SPM aggregates. A greater degree of particularization can be seen in SPM samples treated with colloid particles.

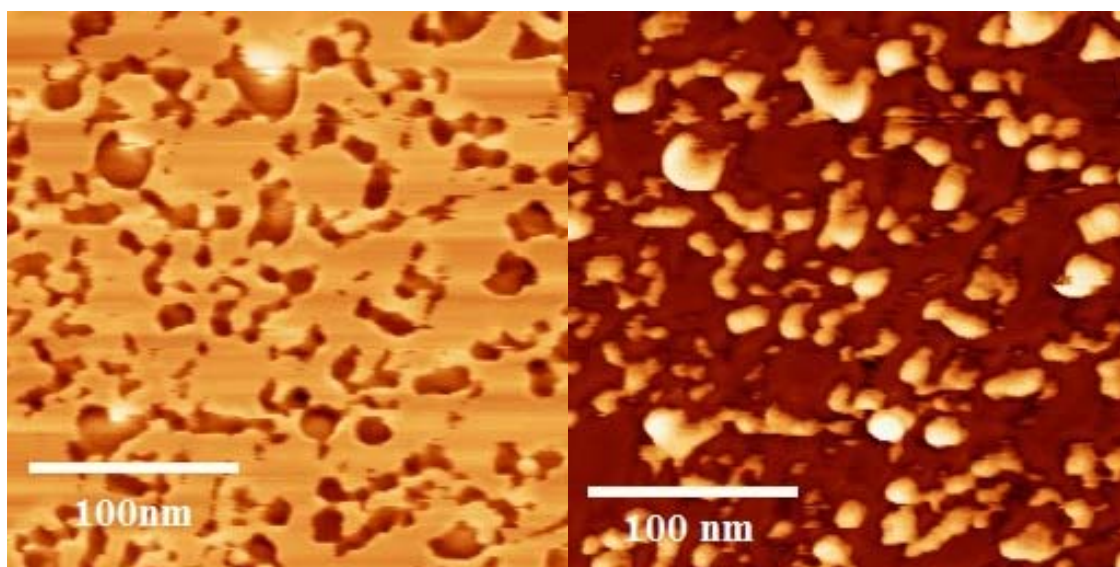


Fig. 5. AFM images of SPM treated with Au NPs deposited on HOPG after 15 min deposition time, scanned area  $250 \times 250 \text{ nm}^2$ ; a) - 2D topography, b) - 2D phase view.

### 3.4 Influence of Au NPs on ATPase activity

The influence of Au NPs within the concentration range from  $10^{-10}$  –  $5.25 \times 10^{-10}$  M on the ATP hydrolysis catalyzed by SPM  $\text{Na}^+/\text{K}^+$ -ATPase and  $\text{Mg}^{2+}$ -ATPase was investigated, with the aim to find out if proteins retain their functionality in the presence of colloids. In this experiment the medium assay contained 20  $\mu\text{g}$  protein. The catalytic reaction was started by addition of ATP

1 min after the nanoparticles were added into the medium assay and the results are presented in Fig.6.

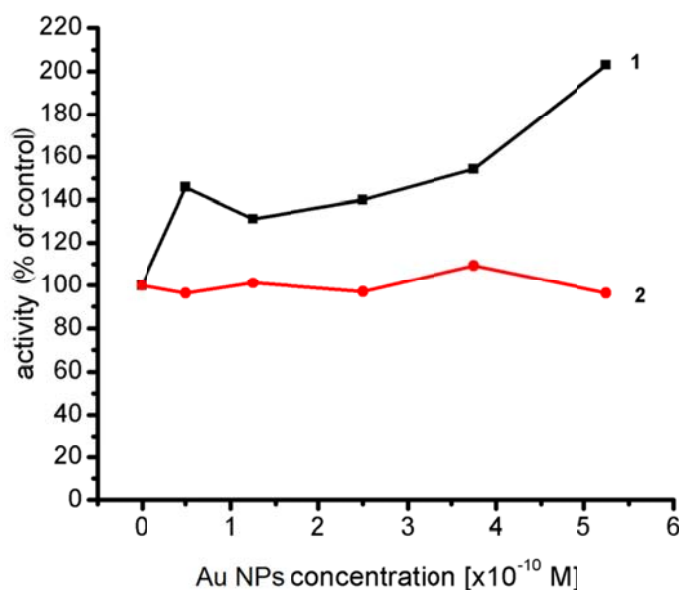


Fig. 6. Influence of Au NPs on Na<sup>+</sup>/K<sup>+</sup>-ATPase (1) and Mg<sup>2+</sup>-ATPase (2) activity after 1 min preincubation.

The results indicated, that the borate capped Au NPs increased the activity of Na<sup>+</sup>/K<sup>+</sup>-ATPase in the concentration dependent manner, compared to the control value without nanoparticles, since the activity of Mg<sup>2+</sup>-ATPase remained constant. Moreover, the increase of the Na<sup>+</sup>/K<sup>+</sup>-ATPase activity was more than 100% in the presence of 5.25x10<sup>-10</sup> M Au NPs.

In the additional experiment the incubation time of SPM with nanoparticles (concentration was 5.25x10<sup>-10</sup> M) was varied from 0.5 min to 120 min. The Na<sup>+</sup>/K<sup>+</sup>-ATPase activity increased for about the same value (100%) in all cases compared with the control value without nanoparticles, since Mg<sup>2+</sup>-ATPase activity reminded unchanged.

Furthermore, an experiment with a constant concentration of nanoparticles (5.3 x 10<sup>-10</sup>M) and a varying the amount of protein (from 5 µg – 40 µg total amount in medium assay) was carried out in order to investigate the trend of activity rise that was shown for Au NPs. The increase of activity for 85 – 110% compared to the control probe containing the same protein concentration without Au NPs was obtained in all cases.

In order to see if the interaction between Au NPs (concentration 5.25x10<sup>-10</sup> M) and SPM Na<sup>+</sup>/K<sup>+</sup>-ATPase altered the enzyme selectivity towards its specific inhibitor, a set of activity measurements was carried out in the presence of ouabain, a selective inhibitor of Na<sup>+</sup>/K<sup>+</sup>-ATPase. Concentration span of ouabain in the assay was from 1x10<sup>-8</sup> M to 10<sup>-5</sup> M. Simultaneously, the inhibition was investigated in the medium assay of the same composition without Au NPs. Results show that the response of the enzymatic activity to the ouabain concentration is biphasic, indicating high and low affinity Na<sup>+</sup>/K<sup>+</sup>-ATPase isoforms (Fig.7). It is clear from the experimental results that the activity vs. ouabain concentration plots in both cases can be represented by the sum of two overlapping sigmoid curves, separated by a plateau as found in our previous work. [26, 31], [32]

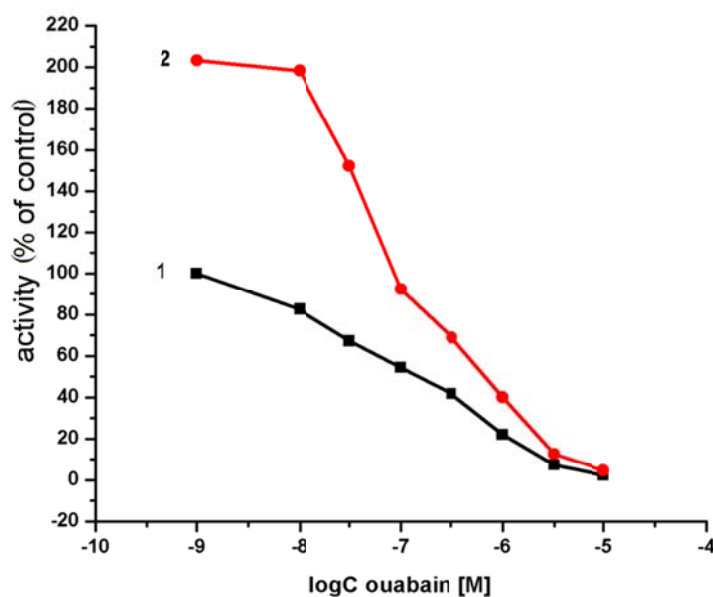


Fig 7. Inhibition of  $\text{Na}^+/\text{K}^+$ -ATPase activity by ouabain in the presence (1) and absence (2) of  $5.25 \times 10^{-10}$  M Au NPs.

The concentration dependent inhibition curves which correspond to high and low affinity inhibitor sites were obtained can be presented as the superposition of two sigmoid curves. Our results show that there was no major change in the  $\text{IC}_{50}$  values of ouabain.  $\text{IC}_{50}$  was found to be  $(5.29 \pm 0.29) \cdot 10^{-7}$  M for high and  $(2.36 \pm 0.29) \cdot 10^{-6}$  M for low affinity binding sites in both cases.

#### 4. Discussion

The position of SPR band of Au NPs is affected by the particle size, shape, inter-particle distance and local dielectric environment of the particles [33]. Since the prepared Au NPs possessed a negative charge due to the adsorbed borate ions, the repulsive forces worked along particles and prevented their aggregation. Previous studies on nanoparticle-protein interactions suggest that adsorption of protein on the gold surface can induce formation of aggregates as a consequence of interaction between the positive surface residue of protein and the negative charge surface layer so the protein molecules constitute bridge among Au NPs [12, 34]. Also, during the formation of an adsorption layer on the Au surface, the anions can be replaced by protein upon adsorption, with the amino acids functional groups (amine and thiol groups) that interact directly with the Au surface [35-38]. Furthermore, the hydrophobic interactions among protein molecules within the protein layer adsorbed on the gold surface cannot be excluded. In the case of Au NPs, where borate anions could be easily replaced by the SPM molecules, a direct binding to the particle surface occurs *via* thiolate ( $-\text{SH}$  group) linkages through the cysteine residues [39], rather than  $-\text{NH}_2$ , which is consistent with the greater affinity of Au for  $-\text{SH}$  compared to  $-\text{NH}_2$ .

Consequently, these interactions can induce changes in the protein structure like a conformation changes, unfolds in protein near the particles surface, etc. The positions of amide I and amide II bands in the FTIR spectra of proteins are sensitive indicator of conformational changes in the protein secondary structure [30]. The amide I band is the sum of overlapping component bands ( $\alpha$ -helix,  $\beta$ -sheet,  $\beta$ -turn and randomly coiled conformation), influenced by their different environment [40], while the amide II band indicates the amount of protein adsorbed on surface. The NPs interactions with SPM lead to the slight displacement and increase intensity of these bands. A probable reason for these changes is the orientation effects of the SPM molecule

during the interaction with gold surface. Nonetheless, it is worth noticing that no major rearrangement of the protein secondary structure upon interaction with gold surface occurred.

AFM measurements enabled us to get information on the topography of membrane-bound proteins with extramembraneous protrusions. The lower domains can be described as the double lipid layer, since the higher domain represents the membrane parts with the high concentration of the transport protein [41],[42]. The results obtained by AFM measurements could imply that the presence of colloid particles caused further membrane fragmentation on a nano scale, resulting in greater effective membrane surface which in turn enables more Na<sup>+</sup>/K<sup>+</sup>-ATPase molecules to hydrolyze ATP, thus creating a stimulation of enzyme activity. It increased either by increasing local enzyme concentration on the particle surface, or simply by revealing more active centers. We also propose that the rise in the activity of SPM Na<sup>+</sup>/K<sup>+</sup>-ATPase may be a consequence of the immobilization of plasma membrane fragments on the surface of the particles. Also, the small surface of the particle in Au NPs might cause the enzyme units to cooperate or perhaps create a local rise in the concentration of substrate and/or cofactors (Mg<sup>2+</sup>, Na<sup>+</sup> and K<sup>+</sup> ions) necessary for the function of the enzyme, thus facilitating its operation.

## 5. Conclusion

Spectrophotometric, FTIR and AFM analysis of borate capped Au NPs – SPM assembly indicated that interactions between NPs and proteine molecules occurred due to the chemical bonding between NPs surface and positive charged cysteine moiety. The selectivity of the enzyme towards its natural inhibitor, ouabain, was preserved and unchanged. We propose that this rises in enzyme activity (observed through biochemical assays) is a result of chemical bonding and spatial reorganization of SPM on the colloid surface (observed through spectroscopic methods) which induced physical fragmentation and improved distribution of SPM aggregates across the colloid particles (seen on AFM).

## Acknowledgements

This study was supported by the Ministry of Education and Science of the Republic of Serbia, Project No. 172023.

## References

- [1] P. Tiwari, K. Vig, V. Dennis and S. Singh, *Nanomaterials* **1**, 31 (2011)
- [2] B. D. Chithrani, A. A. Ghazani and W. C. W. Chan, *Nano Lett.* **6**, 662 (2006)
- [3] H. M. E. Azzazy and M. M. H. Mansour, *Clin. Chim. Acta* **403**, 1 (2009)
- [4] T. C. Yih and M. Al-Fandi, *J. Cell. Biochem.* **97**, 1184 (2006)
- [5] E. E. Connor, J. Mwamuka, A. Gole, C. J. Murphy and M. D. Wyatt, *Small* **1**, 325 (2005)
- [6] Y. Pan, S. Neuss, A. Leifert, M. Fischler, F. Wen, U. Simon, G. Schmid, W. Brandau and W. Jahnen-Dechent, *Small* **3**, 1941 (2007)
- [7] A. Vujačić, V. Vodnik, G. Joksić, S. Petrović, A. Leskovic, B. Nastasijević and V. Vasić, *Dig. J. Nanomat. and Biostr.* **6**, 1367 (2011)
- [8] J. Ralston, J. F. Zhou, D. A. Beattie and R. Sedev, *Langmuir* **23**, 12096 (2007)
- [9] S. Ariyasu, A. Onoda, R. Sakamoto and T. Yamamura, *Dalton Trans* **19**, 3742 (2009)
- [10] D. Li, Q. He, Y. Cui, L. Duan and J. Li, *Biochem. and Biophys. Res. Commun.* **355**, 488 (2007)
- [11] R. Kumar, A. N. Maitra, P. K. Patanjali and P. Sharma, *Biomaterials* **26**, 6743 (2005)
- [12] O. Horovitz, G. Tomoaia, A. Mocanu, T. Yupsanis and M. Tomoaia-Cotisel, *Gold Bulletin* **40**, 213 (2007)
- [13] N. Thi Ha Lien, L. Thi Huyen, V. Xuan Hoa, C. Viet Ha, N. Thanh Hai, L. Quang Huan, F. Emmanuel, D. Quang Hoa and T. Hong Nhung, *Adv. in Nat. Sci. Nanosci. and Nanotech.*

- 1**, 25009 (2010)
- [14] N. Wangoo, K. K. Bhasin, S. K. Mehta and C. R. Suri, *J. Colloid and Interface Sci.* **323**, 247 (2008)
- [15] J. Noble, S. Thobhani, S. Attree, R. Boyd, N. Kumarswami, M. Szymanski and R. A. Porter, *J. Immunol. Meth.* **356**, 60 (2010)
- [16] K. Leung, Molecular Imaging and Contrast Agent Database [database online]. Bethesda (MD): National Library of Medicine, National Center for Biotechnology Information (2011)
- [17] H. J. Apell and S. J. Karlish, *J. Memb. Biol.* **180**, 1 (2001)
- [18] P. Lucchesi and K. Sweadner, *J. Biol. Chem.* **266**, 9327 (1991)
- [19] A. K. Nagy, T. A. Shuster and A. V. Delgado-Escueta, *J. Neurochem.* **47**, 976 (1986)
- [20] T. Momić, M. Čolović, D. Krstić and V. Vasić, *Advances in Chemistry Research*, Nova Science Publishers Inc., New York (2011)
- [21] V. Vasić, T. Momić, M. Petković and D. Krstić, *Sensors* **8**, 8321 (2008)
- [22] B. J. Shaw and R. D. Handy, *Environment International* **37**, 1083 (2011)
- [23] C. Ramsden, T. Smith, B. Shaw and R. Handy, *Ecotoxicology* **18**, 939 (2009)
- [24] B. R. Nechay, *Arthritis & Rheumatism* **23**, 464 (1980)
- [25] M.Ie. Roman'ko, L.S. Rieznichenko, T.H. Hruzina, S. M. Dybkova, Z.R. Ul'berh, V.O. Ushkalov, A. M. Holovko, *Ukr. Biokhim. Zh.* **81**, 70 (2009)
- [26] V. Vasić, D. Jovanović, D. Krstić, G. Nikezić, A. Horvat, L. Vujisić and N. Nedeljković, *Tox. Lett.* **110**, 95 (1999)
- [27] M. J. Hostetler, J. J. Stokes and R. W. Murray, *Langmuir* **12**, 3604 (1996)
- [28] Y. Sahoo, H. Pizem, T. Fried, D. Golodnitsky, L. Burstein, C. N. Sukenik and G. Markovich, *Langmuir* **17**, 25 (2001)
- [29] F. N. Crespilho, F. C. A. Lima, A. r. B. F. da Silva, O. N. Oliveira Jr and V. Zucolotto, *Chem. Phys. Lett.* **469**, 7907 (2009)
- [30] A. Dong, P. Huang and W. S. Caughey, *Biochemistry* **31**, 182 (1992)
- [31] D. Krstić, N. Tomić, K. Krinulović and V. Vasić, *J. Enz. Inh. Med. Chem.* **21**, 471 (2006)
- [32] D. Krstić, K. Krinulović, V. Spasojević-Tišma, G. Joksić, T. Momić and V. Vasić, *J. Enz. Inh. Med. Chem.* **19**, 409 (2004)
- [33] S. Underwood and P. Mulvaney, *Langmuir* **10**, 3427 (1994)
- [34] S. H. Brewer, W. R. Glomm, M. C. Johnson, M. K. Knag and S. Franzen, *Langmuir* **21**, 9303 (2005)
- [35] D. V. Leff, L. Brandt and J. R. Heath, *Langmuir* **12**, 4723 (1996)
- [36] Y. C. Sasaki, K. Yasuda, Y. Suzuki, T. Ishibashi, I. Satoh, Y. Fujiki and S. Ishiwata, *Biophys. J.* **72**, 1842 (1997)
- [37] A. Gole, C. Dash, V. Ramakrishnan, S. R. Sainkar, A. B. Mandale, M. Rao and M. Sastry, *Langmuir* **17**, 1674 (2001)
- [38] W. Shenton, S. A. Davis and S. Mann, *Adv. Mater.* **11**, 449 (1999)
- [39] K. Naka, H. Itoh, Y. Tampo and Y. Chujo, *Langmuir* **19**, 5546 (2003)
- [40] P. Schwinté, J. C. Voegel, C. Picart, Y. Haikel, P. Schaaf and B. Szalontai, *J. Phys. Chem.* **105**, 11906 (2001)
- [41] H.-J. r. Apell, J. Colchero, A. Linder, O. Marti and J. r. Mlynek, *Ultramicroscopy* **42-44**, 1133 (1992)
- [42] J. Jiang, X. Hao, M. Cai, Y. Shan, X. Shang, Z. Tang and H. Wang, *Nano Lett.* **9**, 4489 (2009)